lished a well-defined line which could easily be extrapolated to zero pressure. However, the values of f_2^0/x_2 obtained from the analytical calculations did not establish good lines and it is believed considerable error resulted from the interpretation given by the program to points at very low concentrations. For this reason, the values of Henry's constant obtained graphically are considered to be the more reliable.

Glossary

f_2^0	fugacity of solute at zero pressure
K_{N_2}	equilibrium ratio for nitrogen
$K_{i\text{-}C_5H_{12}}$	equilibrium ratio for isopentane
M	molecular weight
n	refractive index
n_L	refractive index of liquid
n_V	refractive index of vapor
P	pressure
R_{LL}^0	Lorentz-Lorenz molal refractivity at zero pressure
V_L	molal volume of liquid
V_V	molal volume of vapor
x	mole fraction of component in liquid phase
x_2	mole fraction of solute in liquid phase
y	mole fraction of component in vapor phase
ρ	molal density

Literature Cited

(1) Benedict, M., Webb, G. B., Rubin, L. C., *J. Chem. Phys.*, **8**, 334 (1940).
(2) Besserer, G. J., Robinson, D. B., *Can. J. Chem. Eng.*, **49**, 651 (1971).
(3) Besserer, G. J., Robinson, D. B., *J. Chem. Eng. Data*, **18**, 298 (1973).
(4) Besserer, G. J., Robinson, D. B., *J. Chem. Eng. Data*, **20**, 93 (1975).
(5) Besserer, G. J., Robinson, D. B., *J. Chem. Eng. Data*, **20**, 157 (1975).
(6) Bishnoi, P. R., Miranda, R. D., Robinson, D. B., *Hydrocarbon Process.*, **53**, 197 (1974).
(7) Christiansen, L. J., Fredenslund, A., *AIChE J.*, **21**, 49 (1975).
(8) Kalra, H., Robinson, D. B., Besserer, G. J., *J. Chem. Eng. Data*, submitted, June, 1976.
(9) Keilich, S., *Physica* (*Utrecht*), **28**, 1116 (1962).
(10) Smyth, C. P., Engel, E. W., Wilson, Jr., E. B., *J. Am. Chem. Soc.*, **51**, 1736 (1929).

Received for review July 30, 1976. Accepted February 9, 1977. The financial support received from the Canadian Natural Gas Processing Association and the Research Council of Alberta is gratefully acknowledged. Aage Fredenslund provided the computer program for carrying out the consistency tests.

Vapor–Liquid Equilibrium of Petroleum Fractions Single Fraction and Binary Systems

Hamed H. Hamza*† **and Paul G. Mikolaj**
Department of Chemical and Nuclear Engineering, University of California, Santa Barbara, California 93106

Narrow boiling petroleum fractions were obtained from a straight run cut (30–350 °C) and were thoroughly characterized. The vapor pressure of the narrow boiling petroleum fractions was measured in an equilibrium cell and compared with that of the corresponding pure component at different temperatures. Considering the petroleum fractions as pseudo-components, the vapor–liquid equilibria of binary systems containing petroleum fractions were studied at subatmospheric pressures. The modified regular solution model was found to represent the resulting activity coefficients.

At the present time, the most widely used correlation to predict the vapor–liquid equilibrium of petroleum fractions is that presented in 1961 by Chao and Seader (*3*). This is because the Chao–Seader correlation predicts the vapor–liquid equilibrium ratios of multicomponent systems from a knowledge of the pure component properties, i.e., from pure "pseudo-components" properties in the case of petroleum fractions.

The most recent trend of vapor–liquid equilibrium correlations uses pure component data together with binary data in the form of experimentally obtained binary interaction parameters (*5, 11*), to predict the vapor–liquid equilibrium of multicomponent systems. Unfortunately, however, these new techniques are not generally applicable to systems containing petroleum fractions. The major difficulty lies not in the ability of the correlation to accommodate petroleum fractions, but rather in establishing the necessary binary interaction parameters. The problem then lies in defining and calculating a binary interaction parameter to be used for petroleum fractions (*10*).

A method has been presented that can allow the generation of binary vapor–liquid equilibrium data for systems containing pseudo-components (petroleum fractions). The experimental data were accurately represented by a modified regular-solution model for liquid-phase activity coefficients.

Experimental Section

The equilibrium still used in this investigation is of the vapor recirculating type (*6, 8, 9*). It is made of glass and designed so that the contactor is self-lagged with its own vapor. The temperature of the liquid in the contactor was measured with an accuracy of ±0.1 °C by a calibrated iron-to-constantan thermocouple. The pressure in the still was measured by an open U-tube mercury manometer and a precision cathetometer. The overall accuracy in the pressure measurements was better than ±0.2 mmHg. A microset electrical manostat was used to control the pressure in the still. The operation of the still was checked with pure single components and a binary system (*7*).

A Hewlett-Packard Model 5750 gas chromatograph (GC), equipped with two flame ionization detectors and connected to a digital integrator, was used in characterization and analysis. Two identical 10 ft long stainless steel columns, packed with 5% OV-101 (dimethyl silicone fluid) on 80/100 Chromosorb W-HP, were used in the analysis. The GC was calibrated using mixtures of known compositions of the petroleum fractions to be analyzed. From the calibrations, it was deduced that the accuracy of the analyses is ±0.3 mole % for F4–F8 and F5–F9 and ±0.5 mole % for n-C_7–F5 and benzene–F5 (*6*).

The four petroleum fractions used in this study were obtained by distilling a wide-boiling light fraction of a Libyan crude oil called Nafoora. Some of the important properties of the crude oil and the Nafoora light fraction are given in Table I (*6*).

The four petroleum fractions used were characterized by measuring their specific gravity, their content of aromatics,

---

[†] Correspondence concerning this paper should be addressed to H. H. Hamza who is with Fluor Engineers and Constructors, Inc., 3333 Michelson Dr., Irvine, California 92715.

Table I. Analysis of Nafoora Crude Oil

	Distillates						Residue			
	Nafoora light fraction									
	Naphtha	Kerosene jet	Diesel	Light fuel oil	Waxy gas oil	Extra heavy gas oil	Short vacuum	Vacuum	Atmospheric	Whole dry crude
TBP cut point temp, °C, at start	Start	149	232	288	343	454	566^+	454^+	343^+	
TBP cut point temp, °C, at end	149	232	288	343	454	566				
Yield of cut from crude, vol %	11.3	13.0	10.2	11.5	19.7	13.7	20.6	34.3	54.0	100.0
Gravity, °API	62.6	49.3	41.4	37.1	32.4	27.1	16.0	19.8	24.3	34.5
Sulfur, wt %	0.026	0.13	0.23	0.25	0.27		0.51	0.45	0.38	0.30

Table II. Measured Characterization of the Petroleum Fractions

	Temperatures, °C[a]					Volume %		
Fractions	IBP[b]	$T_{50\%}$[c]	FBP[d]	Av mol wt	Specific gravity	Paraffins and naphthenes	Olefins	Aromatics
F4	86.3	124.4	158.0	113.5	0.7325	96	0	4
F5	117.6	149.9	176.9	127.7	0.7512	93	0	7
F8	187.6	216.8	241.6	170.7	0.7862	91	0	9
F9	214.0	237.9	260.8	186.2	0.7990	90	0	10

[a] As obtained using the GC. [b] Initial boiling point. [c] Mid-average temperature. [d] Final boiling point.

Table III. Constants of Antoine's Equation

	Constants of Antoine's equation					
Fraction	*A*	*B*	*C*	ABRD[a] in vp	Range of pressure, mmHg	*N*
F4	7.010 242	1455.761	230.0	0.0080	125–760	12
F5	7.106 002	1602.13	230.0	0.0052	80–760	9
F8	7.283 774	1925.523	220.0	0.0061	90–310	5
F9	6.760 487	1592.815	170.0	0.0033	50–190	4

[a] ABRD = $[\Sigma^N (|\text{Experimental} - \text{Calculated}|)/\text{Calculated}]/N$, N = number of data points.

Table IV. Properties of the Pseudo-components

Fraction	T_c, K	P_c, atm	V, cm^3 g-mol^{-1}	δ (cal cm^{-3})$^{1/2}$ at 25 °C	K (°R)$^{1/3}$
F4	572	26.4	155.0	7.68	12.1
F5	599	24.4	170.0	7.74	12.1
F8	672	19.4	217.1	7.87	2.1
F9	688	18.25	233.0	7.93	12.1

paraffins + naphthenes, and olefins (*2*), their boiling-range distribution (*1*), their average molecular weight, and their vapor pressure. Table II contains the pertinent properties of the fractions.

Since the narrow-boiling petroleum fractions were considered as pure pseudo-components, their vapor pressures were determined using the equilibrium apparatus (*6, 8, 9*). The still was operated isobarically, by using the manostat to adjust the pressure to the desired value, and the power input to the heater was used to control the boiling rate. When equilibrium was reached, the temperature, the pressure, and the liquid levels in both the contactor and the vaporizer remained constant.

A nonlinear regression method was then used to fit the vapor pressure data to Antoine's equation:

$$\log P^0 = A - \frac{B}{(t + C)}$$

where P^0 = vapor pressure in mmHg, t = temperature in °C, and A, B, C are constants. The Antoine constants, together with the error in the curve fit (given by the average absolute relative deviation in the vapor pressure), are shown in Table III.

From the measured characterization parameters, the remaining important properties of the petroleum fractions were obtained either by calculations or from published correlations (*4, 6*). They are summarized in Table IV.

Results

The vapor–liquid equilibria of four binary systems involving petroleum fractions were measured under isobaric conditions. The F4–F8 and F5–F9 systems were studied at a pressure of 100 mmHg, and the *n*-heptane–F5 and benzene–F5 at 760 mmHg.

The equilibrium data obtained isobarically included temperatures and liquid phase compositions. The activity coefficients and the vapor compositions were then calculated using eq 1 and 2 below. To apply eq 1 a model must be used to represent the liquid-phase activity coefficients of the components (*11, 12*). The expressions used for the activity coefficients were the van Laar equations, the two-suffix Margules equations, the modified regular-solution equations, and the Wilson equations. Using a nonlinear regression analysis with the experimental isobaric *T–x* data, the parameters of the selected models were then calculated. The method used minimizes the sum of squares of the deviation in the experimental and calculated pressures from the equation,

$$P = x_1\gamma_1 p_1^0 + x_2\gamma_2 p_2^0 \qquad (1)$$

where P is the pressure of the system.

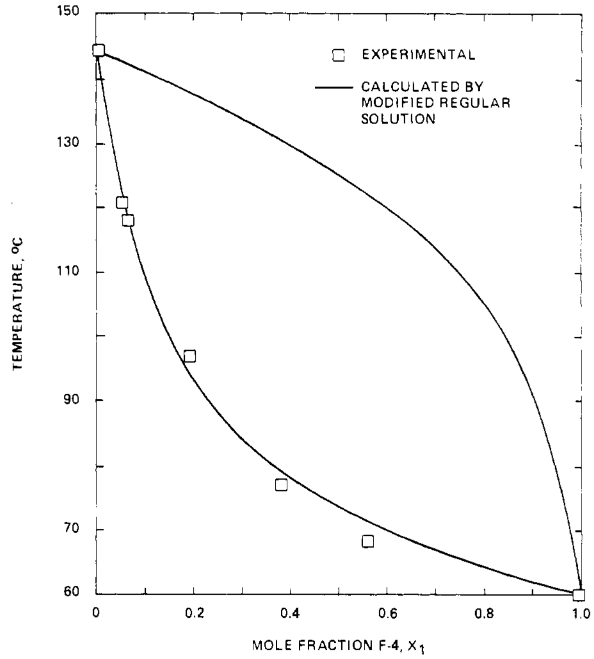

Figure 1. Temperature–composition diagram for the F4–F8 system at 100 mmHg.

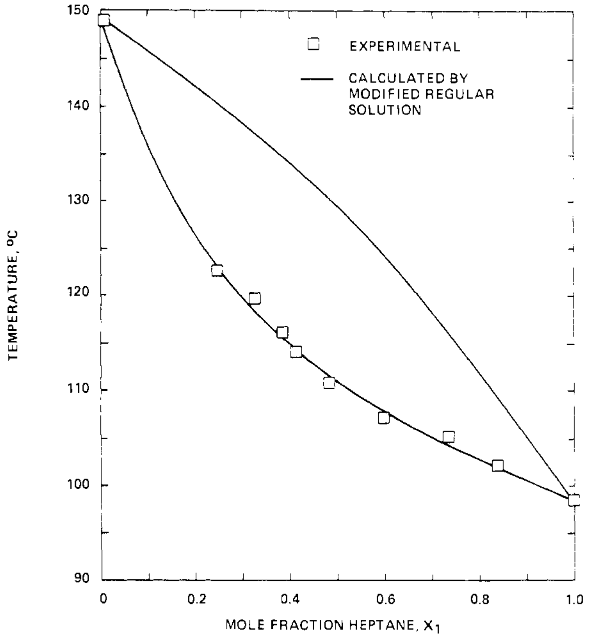

Figure 3. Temperature–composition diagram for the *n*-heptane–F5 system at 760 mmHg.

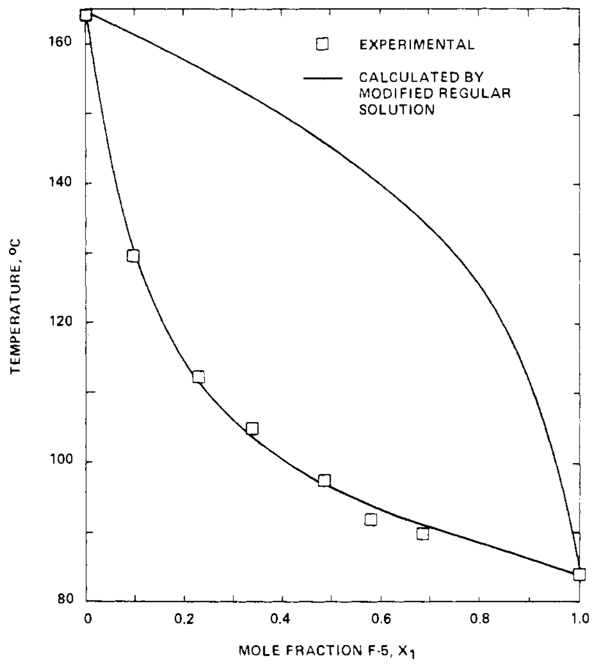

Figure 2. Temperature–composition diagram for the F5–F9 system at 100 mmHg.

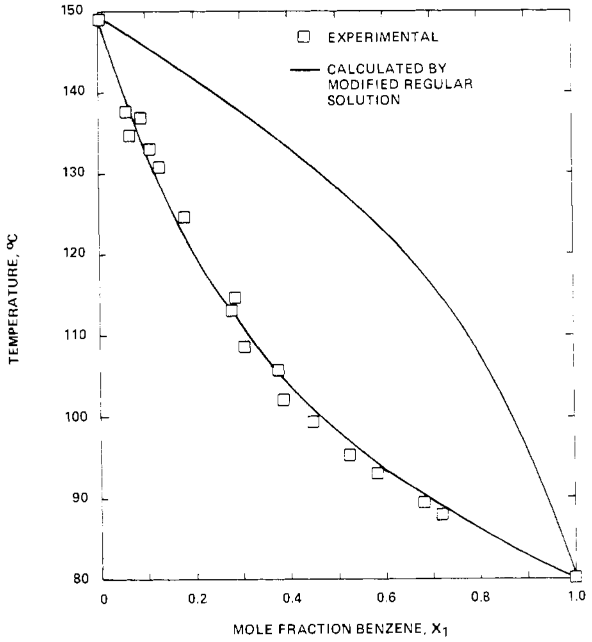

Figure 4. Temperature–composition diagram for the benzene–F5 system at 760 mmHg.

Using the different activity-coefficient models, eq 1 was then solved to calculate the equilibrium temperatures from a knowledge of the total pressure and the liquid-phase compositions. The vapor compositions were simultaneously calculated from a knowledge of the activity coefficients, the calculated temperatures, and the experimental liquid compositions using the equation,

$$Y_i = \frac{x_i \gamma_i p_i^0}{P} \qquad (2)$$

The constants of the Antoine's equation of the *n*-heptane and benzene are obtained from ref 13.

Similarly a set of smooth T–x–y data at equal intervals of x was calculated. When the smoothed T–x data were graphically compared with the experimental data, all four of the activity-coefficient models tested were found to give a good representation of the experimental data. When comparing the RMSD in pressures or temperatures, it was found that the Wilson equations gave better results than the modified regular solution equations, the van Laar equations, and finally the Margules equations. When the γ–x data from the models for the different systems were graphically compared, the differences between them were not large.

Since the regular solution model is presently the most widely used correlating model for petroleum fractions and since the modified regular solution model gives a good representation of the data, this model equation (eq 3) was therefore adopted and used in further analyses. Figures 1–4 show the experimental and

Table V. Summary of VLE Results of the Four Petroleum-Fraction Systems

System	Pressure, mmHg	Mid-average boiling temp, °C		l_{12}	γ_1^{∞}	γ_2^{∞}	G^E,[a] cal mol^{-1} at $x = 0.5$	Acentric factor		
		Component 1	Component 2					ω_1	ω_2	ω_{12}[b]
F4–F8	100	124.4	216.8	0.018	1.51	2.06	100.0	0.365	0.498	0.432
F5–F9	100	149.9	237.9	0.022	1.71	2.46	134.5	0.421	0.588	0.505
n-Heptane–F5	760	98.4	149.9	0.019	1.50	1.70	90.7	0.349	0.421	0.385
Benzene–F5	760	80.1	149.9	−0.008	1.13	1.32	33.1	0.210	0.421	0.316

[a] $G^E = RT \sum_{i=1}^{2} x_i \ln \gamma_i$. [b] $\omega_{12} = \frac{1}{2}(\omega_1 + \omega_2)$.

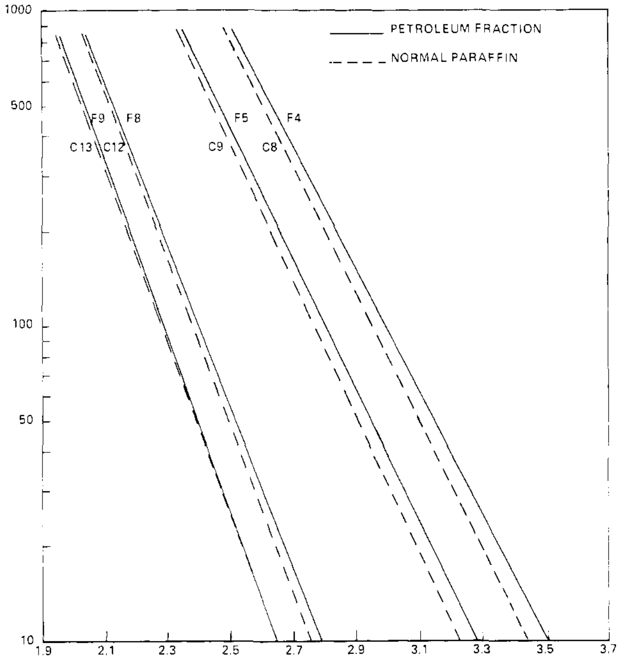

Figure 5. Vapor pressure of F4, *n*-octane, F5, *n*-nonane, F8, *n*-dodecane, F9, and *n*-tridecane.

smoothed vapor–liquid equilibrium data of the four petroleum-fraction systems.

$$RT \ln \gamma_1 = V_1 \phi_2^2[(\delta_1 - \delta_2)^2 + 2l_{12}\delta_1\delta_2] \qquad (3)$$

Discussion and Conclusions

The vapor pressures of four pseudo-components studied in the present investigation were compared with those of pure *n*-paraffins having approximately the same boiling points (*13*) as the mid-average temperatures of the fractions. The vapor pressures of the petroleum fractions and the *n*-paraffins, as calculated from Antoine's equation, are plotted in Figure 5. As shown in the figure, none of the corresponding vapor-pressure lines cross, and this fact can be taken as evidence that the petroleum fractions can be approximated by using vapor pressures of pure components with the same boiling point. This approximation, in fact, is widely used in industrial practice.

A sensitivity analysis was performed to estimate upper and lower limits for l_{12} in the modified regular solution, which would correspond to the variation in the activity coefficients, resulting from possible errors. It was found that the values of l_{12} from the original data, Table V, average close to those limits.

The VLE results of this study summarized in Table V show that whether the nonidealities in the liquid solutions were described by γ^{∞}'s or G^E at $x = 0.5$, the trend in the nonidealities is the same. The F5–F9 system shows the greatest nonideality, followed by F4–F8, *n*-heptane–F5, and benzene–F5. Examining some properties of these four petroleum fraction systems, one finds that none of the properties of the systems seems to offer a quantitative correlation of their nonidealities (*6*).

In calculating the activity coefficients of petroleum-fraction systems using the modified regular-solution equations, the only uncommon parameter that requires specification is l_{12}. Considering Table V, we conclude that the value of l_{12} that is recommended for predicting activity coefficients in nonaromatic petroleum fraction systems is 0.020. However, in the benzene–petroleum fraction systems, due to insufficient data to substantiate any recommendation, the value of l_{12} recommended for such systems is equal to that in a benzene–*n*-paraffin system, with the *n*-paraffin having a boiling point equal to the average temperature of the petroleum fraction. Therefore, for the benzene–F5 system, the value recommended for l_{12} would be −0.005, which is still within the experimental limits set for l_{12} (*6*).

Glossary

F	narrow-boiling petroleum fraction
G^E	excess Gibbs free energy
K	Watson characterization factor
l_{12}	binary interaction $= [RT \ln \gamma_1/V_1\phi_2^2 - (\delta_1 - \delta_2)^2]/2\delta_1\delta_2$
N	number of data points
P	pressure of the system
p^0	vapor pressure
P_c	critical pressure
T	temperature in K, unless otherwise specified
T_c	critical temperature
t	temperature in °C
$T_{50\%}$	mid-average temperature of the fraction, °C
V	molar volume
x	mole fraction in liquid phase
y	mole fraction in vapor phase
VLE	vapor–liquid equilibrium
RMSD	root mean square deviation RMSD $= [\sum^N (\text{experimental} - \text{calculated})^2/N]^{1/2}$
ABRD	average absolute relative deviation ABRD $= [\sum^N (\lvert\text{experimental} - \text{calculated}\rvert)\text{calculated}]/N$

Greek Letters

δ	solubility parameter
γ	liquid-phase activity coefficient
ω	acentric factor
ϕ	volume fraction

Supercripts

E	excess

Subscripts

i	component i

Literature Cited

(1) American Society for Testing and Materials, ASTM-D2887-70T, "Boiling Range Distribution of Petroleum Fractions by Gas Chromatography", *Annu. Book ASTM Stand.*, Part 17, 1072 (1971).

(2) American Society for Testing and Materials, ASTM-D1319-66T, "Hydrocarbon Types in Liquid Petroleum Products by Fluorescent Indicator Adsorption", *Annu. Book ASTM Stand.*, Part 17, 506 (1967).
(3) Chao, K. C., Seader, Y. D., *AIChE J.*, **7**, 598 (1961).
(4) Fenske, M. R., et al., ed., "Technical Data Book—Petroleum Refining", American Petroleum Institute, New York, N.Y., 1966.
(5) Gunn, R. D., *AIChE J.*, **18**, 183 (1972).
(6) Hamza, H. H., "Vapor Liquid Equilibrium of Petroleum Fractions", Ph.D dissertation, University of California, Santa Barbara, 1973.
(7) Hamza, H. H., Mikolaj, P. G., *J. Chem. Thermodyn.*, **7**, 777 (1975).
(8) Hipkin, H., Myers, H. S., *Ind. Eng. Chem.*, **46**, 2524 (1954).
(9) Lodl, S. J., Scheller, W. A., *J. Chem. Eng. Data*, **12**, 485 (1967).
(10) Mikolaj, P. G., Dev, L.,*AIChE J.*, **17**, 343 (1971).
(11) Prausnitz, J. M., "Molecular Thermodynamics of Fluid-Phase Equilibria", Prentice-Hall, Englewood Cliffs, N.J., 1969.
(12) Van Ness, H. C., Byer, S., Gibbs, R. E., *AIChE J.*, **19**, 238 (1973).
(13) Zwolinski, B. J., Wilhoit, R. C., "Handbook of Vapor Pressures and Heats of Vaporization of Hydrocarbons and Related Compounds", API **44**, Publication No. 101, Thermodynamics Research Center, Department of Chemistry, Texas A&M University, College Station, Texas, 1971.

Received for review August 23, 1976. Accepted January 10, 1977. The authors gratefully acknowledge the donors of the Petroleum Research Fund, administered by the American Chemical Society, for the support of this research.

Thermodynamic Properties of Alcohol–Amine Mixtures: Excess Enthalpies of Methanol–Triethylamine and Ethanol–Triethylamine

Abhai Chand and David V. Fenby*
Department of Chemistry, University of Otago, Dunedin, New Zealand

Molar excess enthalpies have been measured for methanol–triethylamine and ethanol–triethylamine at 298.15 K using a Larkin-McGlashan calorimeter. The results are compared with earlier calorimetric measurements and with molar excess enthalpies obtained from isothermal liquid–gas equilibrium studies. For these systems at 298 K, the molar excess Gibbs functions are positive and the molar excess enthalpies and molar excess entropies negative.

There have been several thermodynamic studies of alcohol–amine, liquid and liquid–gas systems: isothermal and isobaric liquid–gas equilibrium (*2-4, 8, 14*), calorimetric (*6, 15, 17*), volumetric (*4, 16, 17*). The alcohol–amine complex formation has been investigated in "inert" solvents (*9, 17*) and in the gas phase (*12*). References to a few spectroscopic studies can be found in the literature cited. While most of this work has been associated with azeotrope formation, some has been concerned primarily with the analysis of the experimental results in terms of intermolecular interactions. In the belief that alcohol systems ". . . may be more immediately amenable to detailed theoretical analysis," Copp and Everett (*3*) included alcohol–amine mixtures in their thermodynamic study of critical phenomena in H_2O–amine mixtures.

Chun and Davison (*2*) measured the vapor pressures of methanol–triethylamine and ethanol–triethylamine at a number of temperatures in the range 283–313 K. From their results they obtained molar excess Gibbs functions G_m^E at each of the temperatures studied, and the molar excess enthalpies H_m^E [$= -\partial(G_m^E/T)/\partial(1/T)$] and molar excess entropies S_m^E [$= (H_m^E - G_m^E)/T$] at 298 K. The H_m^E results obtained by differentiation are in considerable disagreement with earlier calorimetric work (*6*). Given this discrepancy and the appreciable uncertainties in published H_m^E results for methanol–triethylamine and ethanol–triethylamine, we have measured H_m^E for these systems using a calorimeter and carefully purified materials.

Experimental Section

Purification of Materials. In our studies of triethylamine mixtures we have attempted to ensure the removal of CO_2 from the pure liquids by careful degassing.

Triethylamine (B.D.H., Laboratory Reagent) was refluxed over KOH pellets, distilled from KOH, and then fractionally distilled in a column of 15 theoretical plates at a reflux ratio of 20. During these steps, dry, oxygen-free nitrogen was passed through the apparatus and light was excluded. The middle fraction was dried over freshly activated molecular sieve and degassed using the vacuum sublimation apparatus described by Bell et al. (*1*) and then by successive freezing (using dry ice–acetone), pumping, distillation cycles. The degassed liquid was finally distilled under vacuum into ampoules which were stored in the dark. During use, the material was stored over mercury out of contact with air and in the dark. It has been found (*7*) that the vapor pressure of a sample of triethylamine prepared in this way did not change when successive amounts of material were distilled from it. Methanol (Mallinckrodt, Spectrar) and ethanol (B.D.H., Aristar) were dried, degassed, and stored as in the case of triethylamine. Normal hexane (Phillips Petroleum, research grade) and cyclohexane (Phillips Petroleum, research grade), for use in testing the calorimeter, were dried over freshly activated molecular sieve, degassed by vacuum sublimation (*1*), and stored as in the case of triethylamine.

High amplification NMR studies of all materials indicated no proton-containing impurities.

Calorimeter. This was based on the design used by Larkin and McGlashan (*10*) and has been discussed elsewhere (*5*). Recent modifications include the use of a crystal oscillator timer (Forth Instruments Ltd., Model 112) and, following Morcom and Travers (*13*), instead of evacuating the vacuum jacket, the mixing vessel was placed in a polystyrene enclosure which was fitted into the "vacuum" jacket. The experimental procedure has been discussed previously (*5*).

Following the recommendation of the IUPAC Commission on

Table I. Molar Excess Enthalpies H_m^E of Methanol–Triethylamine and Ethanol–Triethylamine at 298.15 K

Methanol–triethylamine		Ethanol–triethylamine	
x	H_m^E, J mol^{-1}	x	H_m^E, J mol^{-1}
0.0633	−711	0.0401	−341
0.1449	−1399	0.1252	−861
0.2065	−1676	0.2232	−1219
0.3783	−2000	0.3099	−1381
0.4062	−1965	0.4035	−1415
0.4837	−1932	0.5167	−1322
0.6073	−1604	0.6645	−1012
0.7051	−1278	0.7318	−849
0.8327	−761	0.9145	−289